Contemporary Topics in Chemical Engineering: Fundamentals, Processes, and Sustainability

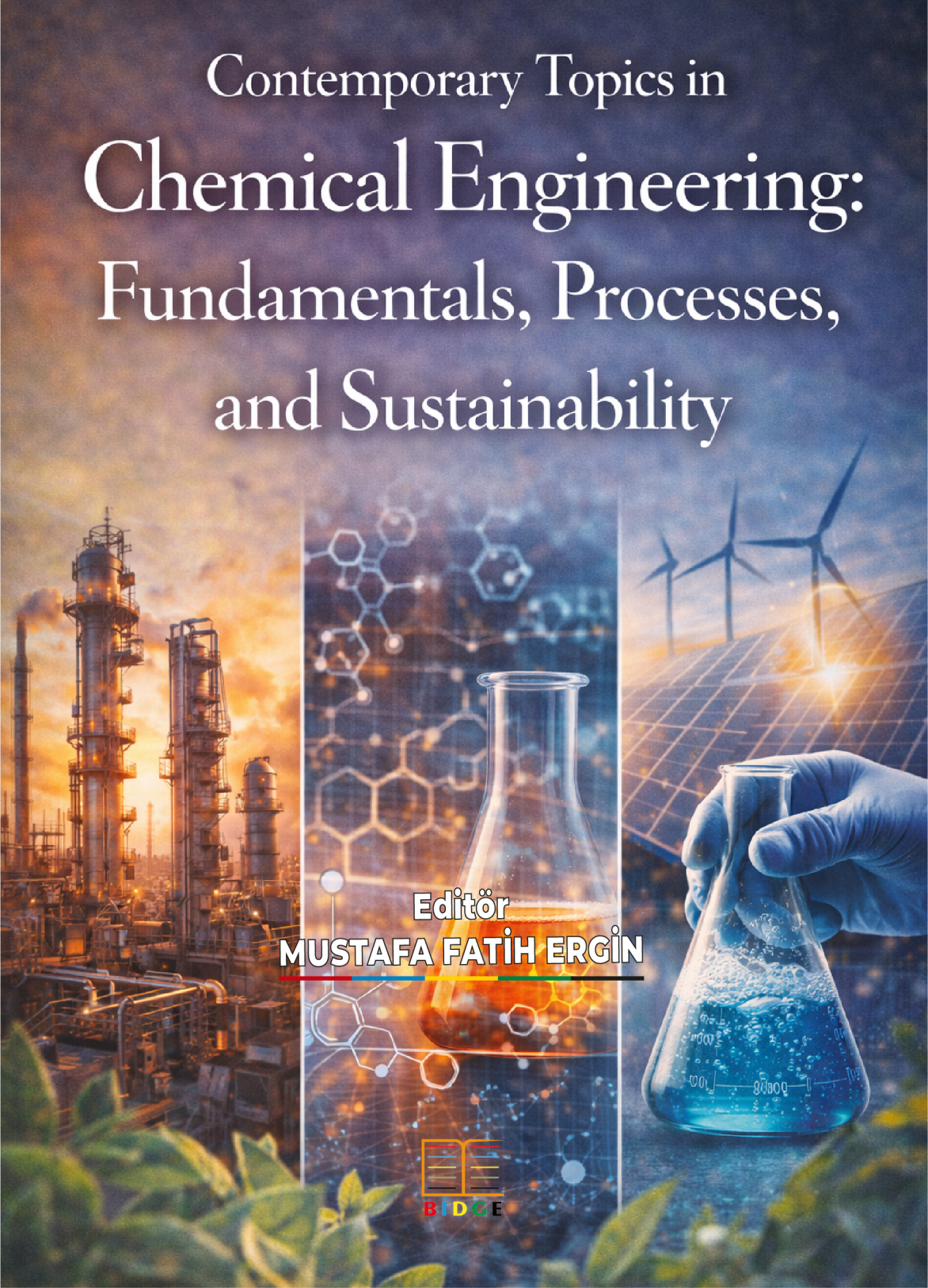

Editör
MUSTAFA FATİH ERGİN

BİDGE

BİDGE Yayınları

Contemporary Topics in Chemical Engineering: Fundamentals, Processes, and Sustainability

Editor: MUSTAFA FATİH ERGİN

ISBN: 978-625-8567-01-4

1st Edition
Page Layout By: Gözde YÜCEL
Publication Date: 2025-12-25
BİDGE Yayınları

Certificate No: 71374

www.bidgeyayinlari.com.tr - bidgeyayinlari@gmail.com
Krc Bilişim Ticaret ve Organizasyon Ltd. Şti.
Güzeltepe Mahallesi Abidin Daver Sokak Sefer Apartmanı No: 7/9 Çankaya / Ankara

Preface

Chemical engineering is a core engineering discipline that integrates fundamental scientific principles with the design and operation of industrial processes. Traditionally grounded in thermodynamics, transport phenomena, reaction engineering, and separation processes, the field has evolved substantially in recent decades. This evolution has been driven not only by technological advances, but also by growing global concerns related to sustainability, energy efficiency, and environmental impact.

The present volume, *Contemporary Topics in Chemical Engineering: Fundamentals, Processes, and Sustainability*, reflects this evolving landscape by bringing together selected topics that capture both the foundational and emerging dimensions of the discipline. Rather than adopting the structure of a conventional textbook or a narrowly focused research monograph, this book follows an integrative approach that links core chemical engineering principles with modern process applications and sustainability-driven challenges.

The chapters in this volume are organized around three interconnected pillars. Fundamental topics, including separation processes, establish the theoretical basis required for effective system design and analysis. Process-oriented contributions illustrate the application of chemical engineering principles in areas such as material synthesis and performance evaluation. Sustainability-focused chapters explore contemporary challenges related to energy transition, alternative fuels, and environmentally responsible process development.

This book is intended for senior undergraduate and graduate students, as well as researchers and professionals seeking a concise yet comprehensive reference on current topics in chemical engineering. By emphasizing conceptual clarity, practical relevance, and sustainability awareness, this volume aims to support both education and professional practice in a discipline that continues to play a central role in addressing complex global challenges.

Assoc. Prof. Dr. M. Fatih ERGIN

İÇİNDEKİLER

CHAPTER 1

METHANOL AS A MARINE FUEL: A TECHNICAL, ECONOMIC, AND ENVIRONMENTAL ASSESSMENT

1. M.Fatih ERGİN[1]
2. Ayfer ERGİN[2]

Introduction: Energy Transition and Paradigm Shift in Maritime

In today's world, where approximately 80-90% of global trade is conducted via sea routes, the maritime sector constitutes the cornerstone of the global economy (Ergin & Ergin, 2023; Ergin & Sandal, 2023; Sandal & Ergin, 2023; UNCTAD, 2024). In this respect, the sector stands out as the most energy-efficient mode of transport, enabling the movement of goods on a global scale with the lowest unit energy input (IEA, 2020; Wu & Lin, 2025). However, this massive logistical operation brings with it a significant environmental cost. The sector consumes approximately 330 million

[1] Assoc. Prof. Dr., Engineering Faculty, Department of Chemical Engineering, Istanbul University-Cerrahpaşa, 34320 Avcılar, Istanbul, Türkiye, Orcid: 0000-0003-4158-368X
[2] Assoc. Prof. Dr., Engineering Faculty, Department of Maritime Transportation Management Engineering, Istanbul University-Cerrahpaşa, 34320 Avcılar, Istanbul, Türkiye, Orcid: 0000-0002-6276-4001

tons of fossil fuel annually and is responsible for about 3% of global anthropogenic carbon dioxide (CO_2) emissions, 14–31% of NOx, and 4–9% of SOx (Deniz & Zincir, 2016; ERGİN & ERGİN, 2018; Kang, 2021).

This energy architecture, built on heavy fuel oil (HFO) and marine gas oil (MGO) throughout the 20th century, entered a radical transformation process in the first quarter of the 21st century. The International Maritime Organization (IMO) adopted MARPOL Annex VI to reduce emissions, enforcing global limits for SOx and NOx (Deniz & Zincir, 2016). Furthermore, the IMO's revised 2023 Greenhouse Gas (GHG) Strategy, which sets a target of reaching "net-zero" emissions around 2050, alongside energy efficiency mandates (EEDI, SEEMP, CII), is forcing the sector to decarbonize at an unprecedented speed (Ammar & Seddiek, 2017; Bilgili & Ölçer, 2024; Joung, Kang, Lee, & Ahn, 2020; Kang, 2021). In addition to these global goals, the European Union's "Fit for 55" package and the *FuelEU Maritime* regulation, which entered into force in 2025, are making the use of fossil fuels financially more punitive with each passing year.

At this historical crossroad, methanol (CH_3OH) stands out, particularly due to its technical feasibility and emission reduction potential (Parris, Spinthiropoulos, Ragazou, Giovou, & Tsanaktsidis, 2024). Requiring no cryogenic storage and capable of being integrated into existing port infrastructure with minimal modification, methanol is viewed as a low-risk investment for shipowners in an era of uncertainty (Ellis & Tanneberger, 2015; Ford, 2012). From an environmental perspective, methanol use has the potential to reduce SOx emissions by 99%, PM emissions by 95%, and NOx emissions by up to 76% (Ammar, 2019; Deniz & Zincir, 2016). However, while the life cycle emissions of fossil-based (grey) methanol remain at levels similar to traditional fuels, the transition to renewable production pathways such as bio-

methanol and e-methanol is critical for meeting climate goals (Ellis & Svanberg, 2018; Mayer et al., 2016; Svanberg, Ellis, Lundgren, & Landälv, 2018).

Economically, (Wu & Lin, 2025) note that while the use of e-methanol increases operating costs in the initial years, its long-term competitiveness increases with the introduction of carbon pricing (Wu & Lin, 2025). On the other hand, methanol's low flash point (~11 °C) and toxicity characteristics (risks of vapor inhalation or skin contact) require special regulations in safety management, such as double-walled piping circuits, inert gas systems, and advanced fire detection technologies within the framework of the IGF Code (Bilgili, 2023; Svanberg et al., 2018; Verhelst, Turner, Sileghem, & Vancoillie, 2019).

Despite all these challenges, 2025 data confirms the shift. Container shipping giants (Maersk, CMA CGM, COSCO, ONE) have turned to methanol dual-fuel vessels rather than LNG when renewing their fleets. This transformation is not limited to ship technology; the signing of "Green Corridor" agreements in major hubs like Shanghai has triggered a simultaneous transformation of fuel bunkering infrastructure. However, the fact that ship orders are increasing faster than finalized green methanol production investments (FID) brings with it a serious **"Supply Gap"** risk. This shift in order books and the supply-demand imbalance indicate that methanol is positioned not just as a "transition fuel," but as a long-term "destination fuel" with manageable risks. This chapter aims to analyze the rise of methanol in the maritime industry in depth, covering its technical, economic, and operational dimensions.

Energy Density and the Tank Volume Paradox

For naval architects and operators, the value of a fuel is a function of its energy density, storage ease, material compatibility, and operational safety. Methanol is a chemical with the simplest

alcohol structure (CH_3OH); it is colorless, water-soluble, and liquid at ambient temperatures. This physical state is its most fundamental advantage over cryogenic fuels like LNG (-162°C) and Hydrogen (-253°C), which require high investment costs. Its ability to be stored in non-pressurized tanks provides flexibility in general ship design (Ellis & Tanneberger, 2015).

The Volumetric Penalty and Thermodynamic Constraints

The greatest handicap of methanol use in shipping is its energy density. While the Lower Heating Value (LHV) of traditional diesel fuel is 42.5 MJ/kg, for methanol, this value is 20.1 MJ/kg. This thermodynamic reality leads to a structural problem in ship design termed the "Volumetric Penalty."

A ship desiring the same endurance range requires methanol tanks approximately 2.2 to 2.5 times larger than conventional fuel tanks (**Figure 1**). For example, for an ultra-large container ship with a range of 15,000 nautical miles, this means thousands of cubic meters of additional volume and potentially the loss of hundreds of containers (TEU) (Ammar, 2019).

***Figure 1**. Comparison of HFO and Methanol tank volume requirements for equivalent energy content.*

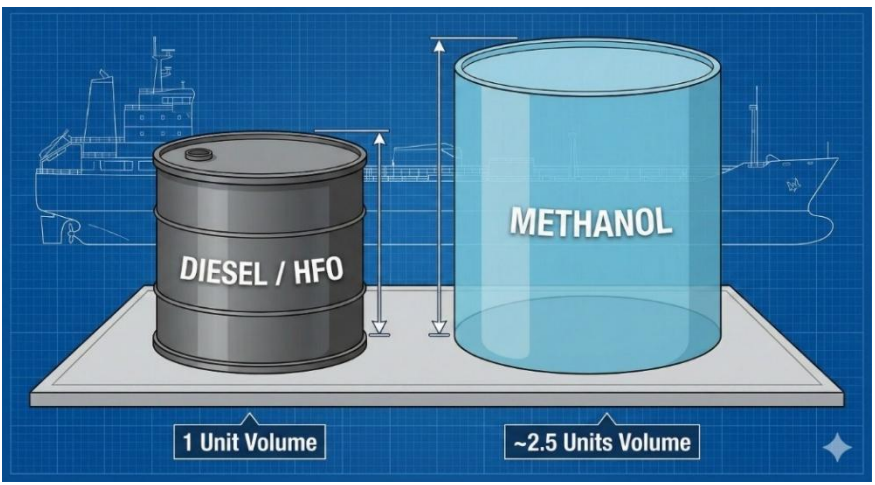

However, the fact that methanol is liquid partially mitigates this disadvantage. While LNG tanks (Type-C cylindrical or prismatic) create large "dead volumes" within the ship, methanol tanks can be integrated into the ship's structure (integral tanks). Ballast tanks, cofferdam spaces, or geometrically difficult areas at the ship's bow/stern can be utilized as methanol storage(Cheenkachorn, Poompipatpong, & Ho, 2013; Deniz & Zincir, 2016). This design flexibility minimizes the negative impact of the volumetric disadvantage on cargo carrying capacity.

Material Compatibility and Corrosive Properties

The physicochemical structure of methanol has a decisive effect on materials used in ship piping systems. Methanol can react aggressively with materials such as aluminum, titanium, and galvanized steel, causing corrosion (Del Pozo, Cloete, & Álvaro, 2022). It also has the property of dissolving certain gaskets and sealing elements (elastomers). Therefore, MAN (2015) reports state that carbon steel is incompatible with methanol; recommending the use of inorganic zinc silicate coatings or stainless steel in fuel tanks, and appropriate alloys in piping circuits (Diesel, 2014).

Flash Point and Fire Characteristics

Methanol has a flash point of approximately 11-12°C **(Table 1)**. This low flash point places the fuel under the scope of the IMO IGF Code (International Code of Safety for Ships Using Gases or Other Low-flashpoint Fuels) and mandates special safety measures such as "double-walled piping circuits" (Bilgili, 2023; Committee, 2016; Verhelst et al., 2019).

The most critical issue regarding safety is the characteristic of the methanol flame (Cheng, Cheung, Chan, Lee, & Yao, 2008; Deniz & Zincir, 2016; El Gohary & Ammar, 2016; Yao et al., 2008). When methanol burns, it does not produce soot and emits a pale blue flame that is nearly invisible in daylight (Deniz & Zincir, 2016). This

makes detection by the human eye or standard optical smoke detectors impossible. To manage this risk, Infrared (IR) Flame Detectors and thermal cameras are mandatory on methanol-fueled ships instead of standard detectors(Wu & Lin, 2025).

Conversely, methanol's complete miscibility with water provides a significant advantage in fire response. Unlike hydrocarbon fires, methanol fires can be extinguished by dilution using copious amounts of water, which limits operational fire risk (Machiele, 1987; Parris et al., 2024).

Consequently, standard visual fire confirmation is obsolete; emergency response protocols must be revised to mandate the use of handheld thermal imaging cameras (TIC) and specialized Personal Protective Equipment (PPE) designed for chemical thermal hazards.

Table 1. *Comprehensive Technical Comparison of Marine Fuels.*

Parameter	Unit	HFO	MGO	LNG	Methanol	Ammonia
Molecular Formula	-	$C_nH_{1.8n}$	$C_{12}H_{23}$	CH_4	CH_3OH	NH_3
Boiling Point	°C	>300	180-360	-162	65	-33
Density	kg/m³	991	890	450	798	682
LHV (Mass)	MJ/kg	40.2	42.7	50.0	19.9	18.6
LHV (Volumetric)	MJ/L	39.8	38.0	22.5	15.8	12.7
Flash Point	°C	>60	>60	-136	11-12	-
Auto-ignition Temp.*	°C	250-400	250	580	460-470	651
Sulphur Content	%	<0.5	<0.1	0	0	0
Storage Pressure**	Bar	Atm.	Atm.	Atm.	Atm.	~10 Bar / Cold

Production Pathways and Sustainability Spectrum: "The War of Colors"

The environmental legitimacy of methanol depends entirely on its production method. The "Well-to-Wake" (WtW) emissions of

fossil-based (grey) methanol can be similar to or higher than traditional fuels (Brynolf, Fridell, & Andersson, 2014). In contrast, methanol produced from biomass or renewable electricity (green) offers a carbon-neutral cycle (Svanberg et al., 2018). Wu and Lin (2025) state that although e-methanol is costly in the early years, it will become competitive in the long term with carbon pricing (Wu & Lin, 2025).

As illustrated in Figure 2, grey methanol relies on conventional steam methane reforming (SMR) of natural gas, where CO_2 is directly released to the atmosphere. Blue methanol represents a transitional pathway in which carbon capture and storage (CCS) technologies are integrated into the SMR process to partially mitigate lifecycle emissions. The figure further distinguishes two structurally different green methanol routes: bio-methanol, based on circular biogenic carbon flows derived from biomass and waste streams, and e-methanol, produced through the synthesis of renewable hydrogen and captured CO_2 using renewable electricity. In this sense, Figure 2 functions not merely as a process diagram, but as a conceptual sustainability map that contextualizes the climate implications of fuel-switching decisions in maritime transport.

Figure 2 *below summarizes the production spectrum of methanol ranging from fossil to renewable sources.*

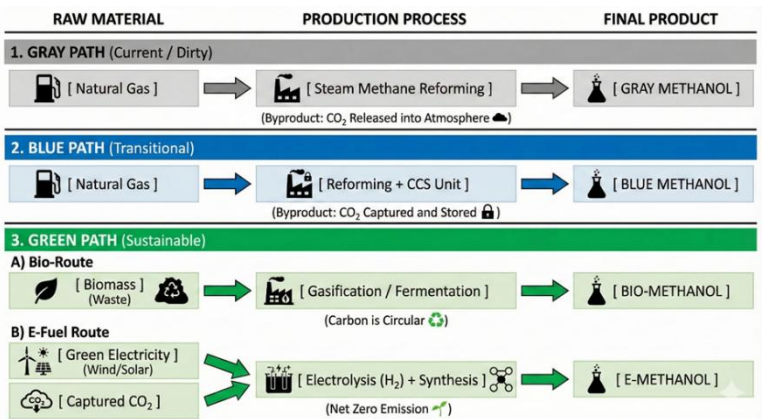

Grey Methanol (Fossil-Based)

Today, approximately 95% of global methanol production is obtained from natural gas (*Steam Methane Reforming - SMR*) or coal (*gasification - especially in China*). The carbon footprint (WtW) of grey methanol is approximately 100-110 gCO_2e/MJ. This value is above that of traditional HFO (~92 gCO_2e/MJ). Thus, operating a ship with grey methanol is more harmful in terms of climate change than operating it with HFO. This situation represents a "transition trap," indicating that production technology must change for methanol to be an environmental solution.

Therefore, a prolonged reliance on grey methanol without a definitive timeline for transition to green variants risks creating a 'climate paradox,' where the maritime sector's shift to alternative fuels inadvertently increases its total Well-to-Wake carbon footprint relative to the HFO baseline.

Blue Methanol (Low Carbon)

"Blue Methanol" is obtained when a Carbon Capture and Storage (*CCS*) unit is added to the grey methanol production process. If 80-90% of the CO_2 released during the SMR process is captured and sequestered underground, WtW emissions can fall below those of HFO. However, fugitive methane emissions during natural gas extraction and transmission can overshadow the environmental gains of this method.

Green Methanol (Renewable)

The sector's ultimate goal is "Green Methanol," which offers a carbon-neutral cycle. As detailed in the comparison of production pathways **(Table 2)**, there are two main sustainable routes:

Bio-Methanol: Produced from forest waste, agricultural residues, municipal waste, or biogas. The carbon released into the atmosphere during combustion is considered circular (carbon

neutral) because it was drawn from the atmosphere during the plant's growth. WtW emission reduction is in the 85-95% range (Kang, 2021; Svanberg et al., 2018).

E-Methanol (Electro-fuel): Green Hydrogen (H_2) is produced by the electrolysis of water using renewable electricity (Wind/Solar). This hydrogen is combined in a reactor with CO_2 captured from industrial stacks or directly from the air (*DAC*). Theoretically, emissions are close to zero (95%+ reduction) (Brynolf et al., 2014; Kang, 2021).

Wu and Lin (2025) state that although the use of e-methanol entails high costs in the initial years (3-4 times that of fossil fuels), its long-term competitiveness will increase with the introduction of global carbon pricing.

Table 2. *Well-to-Wake (WtW) Emission Comparison (Brynolf et al., 2014; Svanberg et al., 2018).*

Fuel Type	Feedstock	WtW Emission (gCO2e/MJ)	Diff. vs HFO
HFO (Reference)	Crude Oil	~92	-
Grey Methanol	Natural Gas	~104 - 110	+13% (Increase)
Blue Methanol	Natural Gas + CCS	~81	-12%
Bio-Methanol	Biomass	~8	-91%
E-Methanol	Wind/Solar	~2	-98%

Technical Assessment: Marine Engines and Fuel Systems

The feasibility of methanol in shipping relies on the maturity of engine technology. Today, two main engine concepts dominate the market: MAN Energy Solutions' *Diesel Cycle* and Wärtsilä's *Otto/Diesel* hybrid approaches.

Two-Stroke Technology: MAN B&W ME-LGIM

The technology that has become the industry standard for large tonnage commercial vessels (Tankers, Containers, Bulk Carriers) is the MAN B&W ME-LGIM (*Liquid Gas Injection Methanol*) engine (Parris et al., 2024; Petrychenko, Levinskyi, Prytula, & Vynohradova, 2023). These engines utilize the high-pressure Diesel combustion principle. Since methanol has a low cetane number (approx. 3-5), it does not ignite spontaneously via compression. The engine first injects a small amount of "Pilot Fuel" (MGO/Diesel, 3-5% of energy) into the cylinder to create an ignition kernel. Immediately after, methanol is injected at high pressure and ignites via the pilot flame.

The heart of the system is the component called the Fuel Booster Injection Valve (FBIV). Methanol is transported to the engine at relatively low pressure (10-13 bar). The FBIV uses hydraulic oil pressure to boost the methanol pressure to 600+ bar right above the cylinder cover. This design reduces safety risks by preventing very high-pressure lines from running along the ship.

Figure 3 below shows a typical low-pressure fuel preparation room. Methanol taken from the service tank is circulated by the "Low-Pressure Pump," its temperature is adjusted in the heat exchanger, and it is sent to the engine via the "Fuel Valve Train" (FVT). The yellow/red lines and drop symbols in the diagram indicate that the system is double-walled and equipped with leak sensors.

Figure 3. *Methanol fuel supply system schematic. Fuel taken from the service tank passes through the low-pressure pump and heat exchanger to reach the Fuel Valve Train (FVT).*

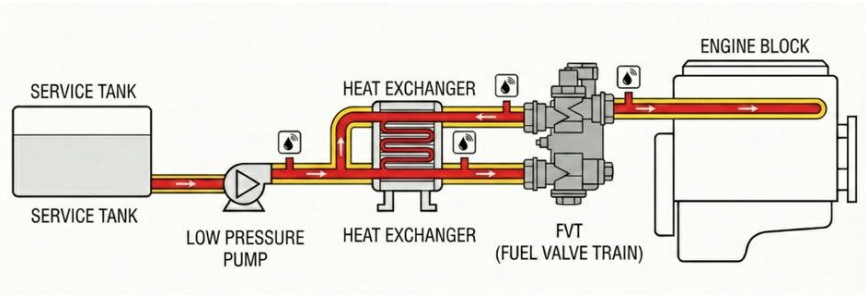

Four-Stroke Technology: Wärtsilä

For smaller vessels and generators, Wärtsilä offers the *Wärtsilä 32 Methanol* engine. This engine can inject methanol via the intake manifold (*port injection*) or directly into the cylinder. Thanks to the lower combustion temperature, NOx emissions can drop to Tier III levels without requiring treatment (or with a simple SCR).

Double-Walled Piping Requirement

Due to methanol being toxic and flammable, all fuel lines within the engine room must be "double-walled." This is a "pipe-in-pipe" design. The inner pipe carries the methanol, while the outer pipe contains any potential leak. The annular space between the two pipes is continuously ventilated or pressurized with inert gas. Sensors placed in this space detect even microscopic leaks instantly and shut down the system (ESD - Emergency Shutdown).

Figure 4 shows a cross-section of a double-walled pipe passing through an engine room bulkhead. The inner orange "Methanol Pipe" carries the main fuel. The outer "Outer Pipe" is protective. A "Leak Detection Sensor" is located in the space between them. This sensor detects methanol vapor or liquid in case of a crack in the inner pipe and triggers an alarm. The "Gland Seal"

ensures the gas tightness of the bulkhead. This structure is the most fundamental safety requirement of the IGF Code.

Figure 4. *Detail of a double-walled pipe passing through an engine room bulkhead. The inner pipe carries fuel, while the outer pipe provides protection and is monitored by a Leak Detection Sensor.*

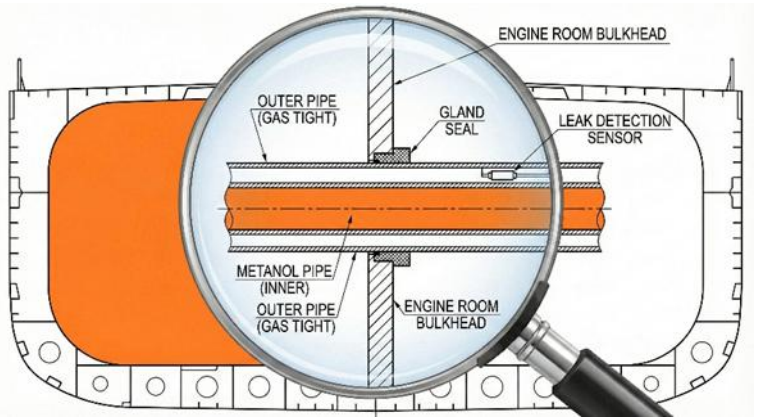

Tank Design and Cofferdam

Methanol tanks can be integrated into the ship's hull (*integral tank*). However, to prevent methanol from leaking into other compartments, all surfaces of the tank must be surrounded by spaces called "Cofferdams." An inert gas (N_2) inlet located at the top of the tank continuously controls the tank atmosphere to prevent explosion risks.

Figure 5 shows a cross-section of a methanol tank. The "Cofferdam" spaces located to the right, left, and top of the tank create a physical barrier between the tank and accommodation or engine room areas. The "Inert Gas (N_2) Inlet" fills the ullage space of the tank with nitrogen gas, reducing the oxygen level below 5% and preventing explosion. The "P/V Valve" balances the tank pressure.

Figure 5. *Methanol tank cross-section. Cofferdam spaces surrounding the tank create a safety barrier preventing fuel from leaking into accommodation or engine room areas.*

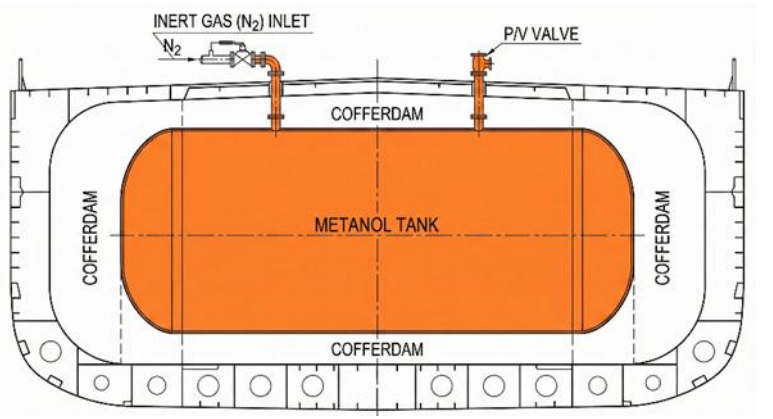

Economic Analysis: Costs, CAPEX, OPEX, and Pooling

Evaluating methanol as an alternative fuel in maritime transport requires a holistic approach that considers not only fuel price but also conversion costs (CAPEX), operating expenses (OPEX), and the opportunity costs introduced by new carbon regulations. Wu and Lin (2025) state that although the use of e-methanol entails high costs in the initial years, it will become competitive in the long term with the introduction of global carbon pricing.

CAPEX (Investment Cost) and Return on Investment

Building a new methanol-fueled ship is **10-15% more expensive** than a conventional ship. This "Green Premium" stems from engine costs, stainless steel or zinc silicate tank coatings, double-walled piping, and gas detection systems. However, this cost is lower than the cryogenic tank investment required for LNG-fueled ships (which entails a 20-25% additional cost).

The cost of converting an existing ship to methanol (*retrofitting*) is approximately **10-11 Million USD** depending on vessel power. Since methanol use eliminates the annual operation and maintenance costs (approx. 1.5 - 1.6 million USD) of the SCR (*Selective Catalytic Reduction*) system mandatory for diesel engines to meet Tier III limits, this investment is projected to amortize itself within approximately **10-12 years**. It is important to note that this estimated retrofit cost of 10-11 Million USD is predicated on large-scale vessels, such as 15,000+ TEU container ships or Aframax tankers, and may vary significantly based on the vessel's age and existing engine architecture.

OPEX (Operating Cost) and Fuel Prices

The most decisive factor in operating costs is fuel price. In a cost-benefit analysis by Wu and Lin (2025), it was modeled that a vessel using a 30% e-methanol blend could become more cost-effective than a conventional fuel vessel after **4.7 years** when carbon taxes (such as the EU ETS) come into play.

- **Grey Methanol:** Priced at approximately 1.2 - 1.5 times that of HFO on an energy-equivalent basis.
- **Green Methanol (E-Methanol):** Production costs are currently very high. It costs 3 to 5 times that of traditional fuels (1000 - 2500 USD/ton).

FuelEU Maritime and "Pooling" Mechanism

To manage the high cost of green fuel, the European Union's *FuelEU Maritime* regulation offers a revolutionary mechanism called "Pooling." This mechanism allows fleet owners to calculate compliance not on a per-ship basis, but on a pool (fleet) basis.

Figure 6. *FuelEU Maritime Pooling Mechanism. The compliance surplus generated by a single ship using E-Methanol can balance the compliance deficit of 70 conventional ships using HFO.*

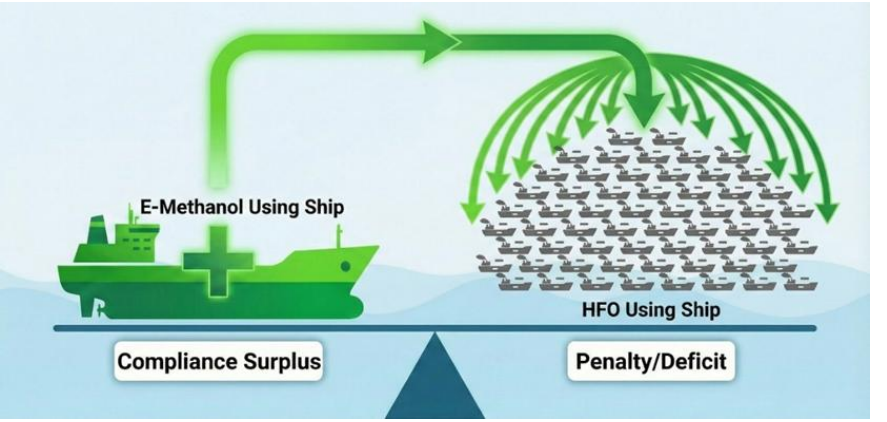

The scale image in **Figure 6** summarizes this mechanism. The "E-Methanol Ship" on the left pan generates a large "Compliance Surplus" because the greenhouse gas intensity of the fuel it burns is far below the regulation limit. On the right pan are 70 "HFO Ships" that are above the limit and would normally pay penalties. However, as shown by the green arrow, the massive surplus obtained from a single green ship is transferred to the pool, covering the "Deficit" of the other 70 ships.

This allows the shipowner to avoid converting all vessels. By adding one or two e-methanol ships to the fleet, the entire fleet can operate within EU waters without penalties. This mechanism ensures economic feasibility by spreading the high cost of green methanol across 70 ships (*cross-subsidization*).

Operational Processes and Bunkering Infrastructure

The fact that methanol exists in a liquid state at atmospheric conditions provides a major cost advantage in storage and transfer infrastructure compared to alternatives like LNG or ammonia. Cryogenic (super-cooled) or high-pressure tanks are not required,

allowing existing infrastructure to be utilized with minimal modification. Thanks to the existing logistics of the chemical industry, methanol is already widely transported in the global supply chain and is scalable and accessible at many major ports.

Bunkering Methods

Methanol bunkering is performed via three main methods depending on vessel type and port infrastructure (**Figure 7**):

Figure 7. *Methanol bunkering methods: Truck-to-Ship (TTS), Ship-to-Ship (STS), and Terminal-to-Ship (TPS).*

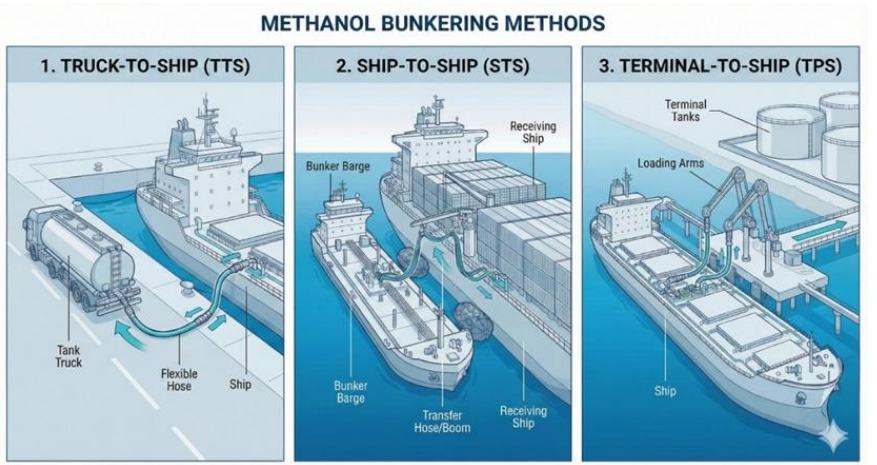

1. **Truck-to-Ship (TTS):** Common for small tonnage vessels, ferries, and pilot projects. It is flexible and requires low investment, but the transfer rate is low.
2. **Ship-to-Ship (STS):** Necessary for large container ships and ocean-going vessels. It allows for high-volume fuel transfer. Methanol bunker barges have entered service in major hubs like Singapore, Rotterdam, and Gothenburg.
3. **Terminal-to-Ship (TPS):** Direct transfer via pipeline from shore to ship. Generally used for tankers or vessels berthing at dedicated methanol terminals.

Port Status (2025 Outlook)

Global ports are responding rapidly to the increasing demand for methanol, expanding bunkering capacities as summarized in **Table 3** (Ellis & Svanberg, 2018). Thanks to existing chemical industry logistics, infrastructure is already scalable at major hubs (Ford, 2012; Svanberg et al., 2018):

Rotterdam: Stands as Europe's methanol hub. OCI Global and other suppliers offer regular barge services. Prices for grey methanol hover in the **300-350 USD/ton** band.

Singapore: The Maritime and Port Authority (MPA) has published methanol bunkering standards (TR 129) and completed licensing procedures, making STS operations routine.

China (Shanghai/Dalian): As the world's largest methanol producer, China has established an aggressive bunkering network using local coal and renewable resources, supported by "Green Corridor" agreements.

Table 3. *Leading Methanol Bunkering Hubs.*

Region	Port	Mode	Status
Europe	Rotterdam	STS / Truck	Active, Green Methanol available
Europe	Gothenburg	STS / Truck	Active (Stena Line operations)
Asia	Singapore	STS	Active, Licensed suppliers
Asia	Shanghai	STS	Green Corridor agreements, Active
USA	Houston	Barge / Terminal	Active, Production hub

Environmental Impact Analysis: Emissions and LCA

The primary reason for methanol's preference in shipping is its superior combustion characteristics compared to fossil fuels (Rachow, Loest, & Bramastha, 2018). Methanol use eliminates SOx emissions almost completely (99%+) due to the lack of sulphur and reduces Particulate Matter (PM) emissions by 90% (Deniz & Zincir, 2016; Parris et al., 2024; Zincir, Deniz, & Tunér, 2019). Additionally,

thanks to its lower combustion temperature, it provides a 60–76% reduction in NOx emissions, facilitating compliance with Tier III standards.

Air Quality (SOx, NOx, PM) and Formaldehyde Risk

Methanol does not contain carbon-carbon or sulphur bonds in its molecular structure. This chemical structure prevents the formation of soot and sulphur oxides after combustion. These features make methanol an excellent fuel for Emission Control Areas (ECA) and port zones.

Regarding NOx emissions, methanol's low adiabatic flame temperature provides an advantage. Combined with water emulsion or EGR (*Exhaust Gas Recirculation*) techniques, it is possible to meet IMO Tier III standards (the strictest NOx limits) without using an expensive after-treatment unit (SCR catalyst).

Furthermore, considering the carcinogenic nature of formaldehyde, strict adherence to Occupational Exposure Limits (OEL) and the installation of continuous gas monitoring systems in engine rooms are imperative to ensure crew long-term health safety.

Note: Formaldehyde Risk A potential side effect of methanol combustion is the formation of Formaldehyde (HCHO) and carbon monoxide (CO). Studies by Zincir, Deniz, and Tuner (2019) have detected that formaldehyde, a toxic and carcinogenic gas, can increase in exhaust gas, especially at low engine loads. Rachow et al. (2018) state that this situation may necessitate the mandatory use of oxidation catalysts (OxCat) in the future.

Greenhouse Gases (GHG) and WtW Analysis

The picture regarding greenhouse gas emissions is more complex. Methanol's climate performance relates to how the fuel is produced (WtT), not just the smoke emitted from the exhaust (TtW). As shown in **Table 4**, using fossil-based (grey) methanol can cause

10-15% higher GHG emissions than HFO in a Well-to-Wake (WtW) analysis. This situation represents a "transition trap," indicating that production technology must change for methanol to be an environmental solution. Consequently, only the "Green" version of methanol (Bio or E-Methanol) is meaningful for long-term climate goals (Svanberg et al., 2018).

Table 4. *Well-to-Wake (WtW) Emission Comparison.*

Fuel	WtT (Production)	TtW (Combustion)	Total WtW (gCO2e/MJ)	Diff. vs HFO
HFO	~14	~78	~92	Reference
Grey Methanol	~35	~69	~104	+13% (Bad)
Blue Methanol	~12	~69	~81	-12% (Improvement)
Bio-Methanol	~8	0*	~8	-91% (Excellent)
E-Methanol	~2	0*	~2	-98% (Net Zero)

Note: Data compiled from the study by Brynolf et al. (2014). Combustion emissions are considered neutral as they are produced from biogenic and atmospheric carbon (Brynolf et al., 2014).

Regulations and Safety Framework

The use of methanol on ships is subject to strict international safety rules due to its low flash point and toxic properties. This framework covers all processes from ship design to crew training.

IMO MSC.1/Circ.1621: The "Interim Guidelines for the Safety of Ships Using Methyl/Ethyl Alcohol as Fuel," published as a supplement to the IGF Code, forms the legal basis for current designs. These guidelines determine tank location, ventilation capacities (30 air changes per hour), explosion risk analyses, and material requirements.

Classification Societies: Organizations like DNV, ABS, and Lloyd's Register certify vessels with "LFL FUELLED" (*Low Flashpoint Liquid*) notations, auditing technical compliance.

STCW and Training: Methanol's toxicity (risk of blindness or death if ingested or inhaled) requires special crew training. Procedures for leak response, gas measurement, and first aid differ completely from those for conventional fuels.

Conclusion and Future Outlook

The maritime sector is on the verge of the most comprehensive energy transition in its history. The technical, economic, and environmental analyses presented in this study reveal that methanol is not just a "transition fuel," but the most pragmatic and scalable "solution partner" for reaching 2050 carbon neutrality goals.

The four strategic pillars shaping methanol's future in the sector can be summarized as follows:

Technological Maturity and Safety: Methanol has evolved from an experimental fuel into an industrial standard. The fuel supply systems detailed in **Figure 3** and the double-walled safety measures shown in **Figure 4** have proven their reliability through thousands of hours of operational data. Technologies offered by engine manufacturers like MAN and Wärtsilä prove that methanol can be burned safely and efficiently.

Infrastructural Flexibility: The fact that methanol is in liquid form is its greatest advantage over competitors. The integral tank designs and *cofferdam* solutions seen in **Figure 5** minimize cargo loss in ship architecture while allowing existing port infrastructure to be used with minimal modification. This significantly lowers the "investment risk" (CAPEX) for shipowners.

Economic Sustainability: Although the production cost (OPEX) of green methanol is currently high, it is not unmanageable. The *FuelEU Maritime Pooling* mechanism analyzed in **Figure 6** and the approaching carbon taxes (ETS) will rapidly close the gap

between fossil fuels and green methanol. Early-moving fleets will gain a competitive advantage through these mechanisms.

Critical Bottleneck - Supply Chain: The biggest risk facing the sector is not technological, but logistical. The imbalance between the rate of increase in ship orders and the commissioning rate of "Green Methanol" production plants (Final Investment Decisions - FID) creates a serious **"Supply Gap"** risk. Over the next 5 years, the "color" of the fuel (Grey or Green?) will be debated more than the engine itself.

Methanol is a candidate to become the **dominant alternative fuel** for the next 20 years, especially in container shipping, Ro-Pax, and short-sea shipping segments. Until competitors like Ammonia—which are "zero-carbon" but carry high toxicity and safety risks—reach technological maturity, methanol remains the most realistic, safe, and technically ready green solution "on the water".

References

Ammar, N. R. (2019). An environmental and economic analysis of methanol fuel for a cellular container ship. *Transportation Research Part D: Transport and Environment, 69*, 66-76.

Ammar, N. R., & Seddiek, I. S. (2017). Eco-environmental analysis of ship emission control methods: Case study RO-RO cargo vessel. *Ocean Engineering, 137*, 166-173.

Bilgili, L. (2023). A systematic review on the acceptance of alternative marine fuels. *Renewable and Sustainable Energy Reviews, 182*, 113367.

Bilgili, L., & Ölçer, A. I. (2024). IMO 2023 strategy-Where are we and what's next? *Marine Policy, 160*, 105953.

Brynolf, S., Fridell, E., & Andersson, K. (2014). Environmental assessment of marine fuels: liquefied natural gas, liquefied biogas, methanol and bio-methanol. *Journal of Cleaner Production, 74*, 86-95.

Cheenkachorn, K., Poompipatpong, C., & Ho, C. G. (2013). Performance and emissions of a heavy-duty diesel engine fuelled with diesel and LNG (liquid natural gas). *Energy, 53*, 52-57.

Cheng, C., Cheung, C. S., Chan, T. L., Lee, S., & Yao, C. (2008). Experimental investigation on the performance, gaseous and particulate emissions of a methanol fumigated diesel engine. *Science of the total environment, 389*(1), 115-124.

Committee, M. S. (2016). International code of safety for ships using gases or other low-flashpoint fuels (IGF code). *International Maritime Organization (IMO)*.

Del Pozo, C. A., Cloete, S., & Álvaro, Á. J. (2022). Techno-economic assessment of long-term methanol production from natural gas and renewables. *Energy conversion and management, 266*, 115785.

Deniz, C., & Zincir, B. (2016). Environmental and economical assessment of alternative marine fuels. *Journal of Cleaner Production, 113*, 438-449.

Diesel, M. (2014). Turbo. Using Methanol Fuel in the MAN B&W ME-LGI Series. In: Copenhagen.

El Gohary, M. M., & Ammar, N. R. (2016). Thermodynamic analysis of alternative marine fuels for marine gas turbine power plants. *Journal of Marine Science and Application, 15*(1), 95-103.

Ellis, J., & Svanberg, M. (2018). SUMMETH–Sustainable Marine Methanol Deliverable D5. 1 Expected benefits, strategies, and implementation of methanol as a marine fuel for the smaller vessel fleet. In.

Ellis, J., & Tanneberger, K. (2015). Study on the use of ethyl and methyl alcohol as alternative fuels in shipping. *Eur. Marit. Saf. Agency, 46*, 1-38.

Ergin, A., & Ergin, M. F. (2023). Alternative Fuels In The Future Of The Maritime Industry. In C. Özalp & S. Bardak (Eds.), *International Theory, Research And Reviews In Engineering* (pp. 147-164). Ankara: Serüven Yayınevi.

ERGİN, A., & ERGİN, M. F. (2018). Reduction of ship based CO2 emissions from container transportation. *International Journal of Computational Experimental Science Engineering, 4*(3), 1-4.

Ergin, A., & Sandal, B. (2023). Mobbing among seafarers: Scale development and application of an interval type-2 fuzzy logic system. *Ocean Engineering, 286*, 115595.

Ford, M. C. (2012). A Masters Guide to: Using Fuel Oil Onboard Ships. *Charles Taylor & Co. Ltd., London*.

IEA, L. (2020). *Tracking transport 2020*.

Joung, T.-H., Kang, S.-G., Lee, J.-K., & Ahn, J. (2020). The IMO initial strategy for reducing Greenhouse Gas (GHG) emissions, and its follow-up actions towards 2050. *Journal of International Maritime Safety, Environmental Affairs, and Shipping, 4*(1), 1-7.

Kang, S. (2021). *Innovation Outlook: Renewable Methanol; International Renewable Energy Agency: Masdar City*. Retrieved from Abu Dhabi,: https://www.irena.org/Publications/2021/Jan/Innovation-Outlook-Renewable-Methanol

Machiele, P. A. (1987). Flammability and toxicity tradeoffs with methanol fuels. *SAE transactions*, 344-356.

Mayer, S., Sjöholm, J., Murakami, T., Shimada, K., Kjemtrup, N., & Kjemtrump, N. (2016). *Performance and emission results from the MAN B&W LGI Low-Speed Engine Operating on Methanol.* Paper presented at the CIMAC Congress.

Parris, D., Spinthiropoulos, K., Ragazou, K., Giovou, A., & Tsanaktsidis, C. (2024). Methanol, a plugin marine fuel for green house gas reduction—a review. *Energies, 17*(3), 605.

Petrychenko, O., Levinskyi, M., Prytula, D., & Vynohradova, A. (2023). Fuel options for the future: a comparative overview of properties and prospects. *Transport systems and technologies*(41), 96-106.

Rachow, M., Loest, S., & Bramastha, A. D. (2018). Analysis of the requirement for the ships using methanol as fuel. *International Journal of Marine Engineering Innovation and Research, 3*(2).

Sandal, B., & Ergin, A. (2023). NAVIGATING UNCERTAINTY: FROM TYPE-1 TO INTERVAL TYPE-2 FUZZY LOGIC IN DECISION MAKING. *Academic Studies in Engineering*, 79.

Svanberg, M., Ellis, J., Lundgren, J., & Landälv, I. (2018). Renewable methanol as a fuel for the shipping industry. *Renewable and Sustainable Energy Reviews, 94*, 1217-1228.

UNCTAD. (2024). *Review of maritime transport, 2024* (978-92-1-002886-8). Retrieved from

Verhelst, S., Turner, J. W., Sileghem, L., & Vancoillie, J. (2019). Methanol as a fuel for internal combustion engines. *Progress in Energy and Combustion Science, 70*, 43-88.

Wu, P.-C., & Lin, C.-Y. (2025). Feasibility and Cost-Benefit Analysis of Methanol as a Sustainable Alternative Fuel for Ships. *Journal of Marine Science and Engineering, 13*(5), 973.

Yao, C., Cheung, C. S., Cheng, C., Wang, Y., Chan, T. L., & Lee, S. (2008). Effect of diesel/methanol compound combustion on diesel engine combustion and emissions. *Energy conversion and management, 49*(6), 1696-1704.

Zincir, B., Deniz, C., & Tunér, M. (2019). Investigation of environmental, operational and economic performance of methanol partially premixed combustion at slow speed operation of a marine engine. *Journal of Cleaner Production, 235*, 1006-1019.

CHAPTER 2

SYNTHESIS OF POLYCARBOXYLATE AND INVESTIGATION OF ITS PERFORMANCE ON CONCRETE

ZEYNEP ÖZSERÇE HASTE[1]

INTRODUCTION

In recent decades, with the development of the construction sector, the importance of concrete and concrete additives has been increasing. Concrete additives consist of three generations: The first generation is commonly produced from ligno sulfonates and the second generation from sulfonated naphthalene formaldehyde or sulfonated melamine formaldehyde. Superplasticizer polycarboxylates (PCEs) are known as third generation concrete additives. Concrete additives are used to increase the performance of concrete by changing some of its properties and/or to make it more economical. Concrete additives contribute to properties such as segregation, workability, consistency, slump, water/cement ratio, compressive strength, setting time, and low cost. Additives are used

[1] Dr. Sivas University of Science and Technology, Chemical Engineering, Orcid: 0000-0001-7783-9515

when preparing fresh concrete and affect properties such as concrete consistency, slump loss, workability, sweating, and setting time(Tan et al., 2018). Polycarboxylates can be modified by using different monomers, reaction temperatures, changes in polymer chain structures, and changing polymer chain length and process conditions. In this way, it allows the synthesis of additives suitable for different needs. Isoprenyl oxy poly(ethylene glycol) (IPEG) is widely used as a monomer in the design and synthesis of PCE materials to reduce the water/cement ratio and for slump protection. IPEG has a hydrophilic group that can be easily polymerized(Lei & Plank, 2014). Methacrylic copolymers of methyl methacrylate and acrylate esters have gained great importance in various fields of industrial applications(Plank, Pöllmann, Zouaoui, Andres, & Schaefer, 2008).

H. Tan (2017) studied the effect of the ester group in the side chain on the adsorption behavior and dispersion of polycarboxylate superplasticizer (PCE) by comparing the performance of two types of PCE. They tested the fluidity, dispersion ability of cement paste and retention ability of PCE to discuss.(Tan, Guo, Ma, Li, & Gu, 2017)

Liu X. (2014) synthesized amide structured polycarboxylate superplasticizers (amide-PCEs) by the amidation reaction between polyacrylic acid (PAA) and amino-terminated methoxy polyethylene glycol (amino-PEG). (Liu et al., 2014b) In order to determine the most suitable synthesis conditions, the effect of amide-PCEs on the amidation rate and flow rate of cement paste, the effects of catalyst dosage, water carrier agent dosage, carboxyl amino ratio, amidation reaction temperature and amidation reaction time were investigated.(Liu et al., 2014)

In this study, IPEG and MMA were synthesized by copolymerization. In order to determine the most suitable synthesis conditions, the effects of reaction temperature, reaction time, and

IPEG/MMA monomer ratios on slump were investigated. As a result of these experiments, the compressive strength of the concrete with the PCE synthesized under the most suitable synthesis conditions obtained, characterization analyses and chemical structure ^{1}H NMR and XRD analysis were examined. In the light of these data, it was determined that the synthesized PCE provided workability, consistency protection, increase in compressive strength and low cost advantages in concrete.

MATERIALS AND METHODS

Materials

Methyl methacrylate (99% purity, Sigma Aldrich, Germany), Isoprenyl oxy poly(ethylene glycol) macromonomer (IPEG) (Liaoning Oxiranchem,China), Ascorbic acid (>99% purity, Sigma-Aldrich Chemie GmbH), cement Votorantim (CEM II A-LL 42.5 R Sivas/Turkey) all substances were used as supplied without further purification.

PCE Synthesis

Copolymerization method was used for PCE synthesis. In experimental studies, a magnetic stirrer heater with temperature accuracy of ±1 ^{0}C and adjustable stirring speed and a reflux cooler connected to it were used. In this study, three different PCEs were synthesized using 100% IPEG, 75% IPEG + 25% MMA, and 50% IPEG + 50% MMA monomer mixtures. For synthesis; the determined amount of monomer is taken into the mixer and 55 ml of distilled water is added. After the monomers are dissolved in the magnetic stirrer basket heater at 400 rpm at 60 ^{0}C, 1 g of ascorbic acid is added as an initiator. For synthesis; the determined amount of monomer is taken into the mixer and 55 ml of distilled water is added. After the monomers are dissolved in a magnetic stirrer basket heater at 400 rpm at 60 ^{0}C, 1 g of ascorbic acid is added as an initiator. 2 M MMA was fed to the system with a dropping funnel for

2, 3 and 4 hours and synthesis was performed at different reaction times. In addition, synthesis was performed at different synthesis temperatures of 40 and 60 ^{0}C.

Concrete Tests

Table1. Concrete recipe (8 dm^3)

Aggregate size(mm)	*Weight (g)*
0-5	*6500*
5-13	*3700*
13-22	*5250*
Cement	*2100*
Water	*1260*

For the concrete mixing process, a U-Test brand pan type concrete mixer was used, In the concrete mixing process, first the aggregates and cement are weighed and put into the mixer, then the weighed water is added and mixed for 1 minute, then the weighed PCE is added and mixed for another 2 minutes. After the concrete mixing process is completed, the first slump is checked immediately and is called slump 1. The concrete that was checked for slump is poured back into the concrete mixer and waited for 30 minutes. In the meantime, the slump hopper, table, and tamping rod are cleaned. After 30 minutes, the concrete is mixed in the mixer for 1 minute and the slump is checked again. This is defined as 30-minute slump. After the concrete mixing process, it is also examined macroscopically whether there is segregation and bleeding, and whether the concrete is pumpable. After the slump tests were completed, concrete samples with acceptable slump values, workability, and consistency were placed in molds for compressive strength testing. Since the concrete samples with a slump value below 9 cm after waiting for 30 minutes would not be suitable for workability, they were placed in molds and not subjected to compressive strength testing. The samples placed in the mold were

removed from the mold after 24 hours and placed in a 20 ± 1 0C heated curing tank. After waiting for 7 days in the curing tank, U-TEST brand UTM-400/S was set at 60 kN, the pressure was set at 0-500 N, and the compressive strength was measured.

RESULTS AND DISCUSSIONS

Effect of PCE Synthesis Time on Slump

In order to examine the effect of the synthesis time for 3, 4 and 5 hours. After the PCE synthesis was completed, concrete tests were performed after waiting at room temperature for 24 hours and cooling. The effect of synthesis time on slump is shown in Figure 1. In the 4 hour synthesis period, the 30 min slump value remained the same and a very good result was obtained in terms of consistency preservation. For this reason, the synthesis period was accepted as 4 hours.

Figure 1. Effect of PCE synthesis time on slump

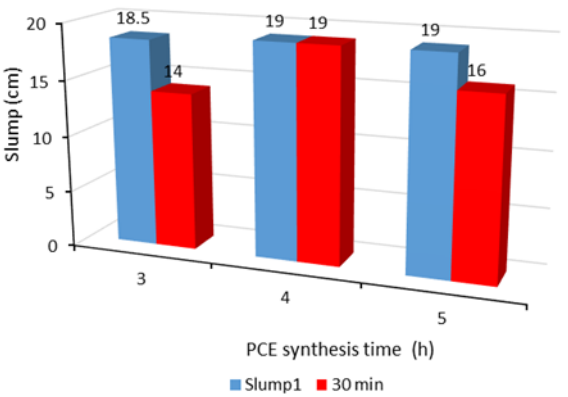

Effect of IPEG Ratio on Slump

In the slump tests performed with different IPEG-MMA percentage ratios, the difference between slump1 and 30 min slump

was obtained by using at least 75% IPEG macromonomer. Since this was a good result obtained in terms of both slump and consistency preservation, 75% IPEG ratio was continued. Figure 2 shows the effect of IPEG ratio on slump.

Figure 2. Effect of IPEG ratio on slump

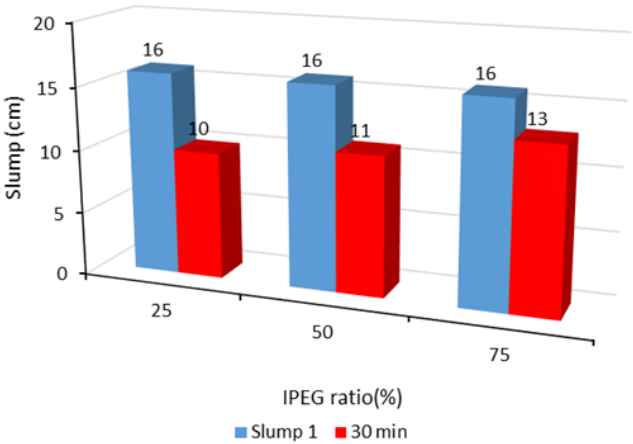

Effect of Synthesis Temperature on Slump and Compressive strength

The effect of PCEs prepared at different synthesis temperatures on concrete efficiency is examined and shown in Figure 3. In the concrete test conducted with PCE synthesized at 40 0C, the initial slump was 18 cm and the slump after 30 minutes was 15 cm, indicating that the concrete was better in terms of workability and consistency preservation. Synthesis at lower temperatures provided energy savings and reduced production costs.

Figure 3.Effect of Synthesis Temperature on Slump

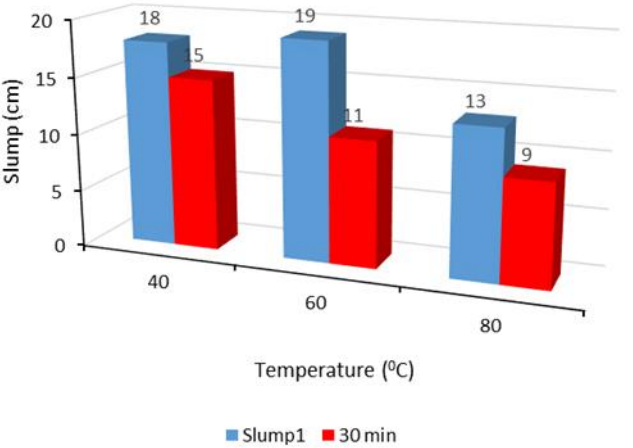

The 7 and 28-day compressive strength test results of PCE synthesized with a synthesis time of 4 hours, an IPEG ratio of 75% and a reaction temperature of 40 0C are given in Figure 4. Characterization analyses were performed with this PCE.

^{1}H NMR

Typically, in the main chain, -CH3 (δ = 0.8 ~ 1.0 ppm), C-CH2-C (δ = 1.0 - 2.0 ppm) signals were given. The strong peak at (δ = 3.30, 3.80 ppm) indicates the side chain ethylene oxide (- CO-CH2). Also, the peak at δ = 4.70 ppm indicates the presence of D2O. All sample products have characteristic functional groups and thus, it can be considered as a relatively complete copolymerization between MMA and IPEG.

Figure 4. 1H NMR spectrum of PCE synthesized with monomer %50 IPEG-%50 MMA

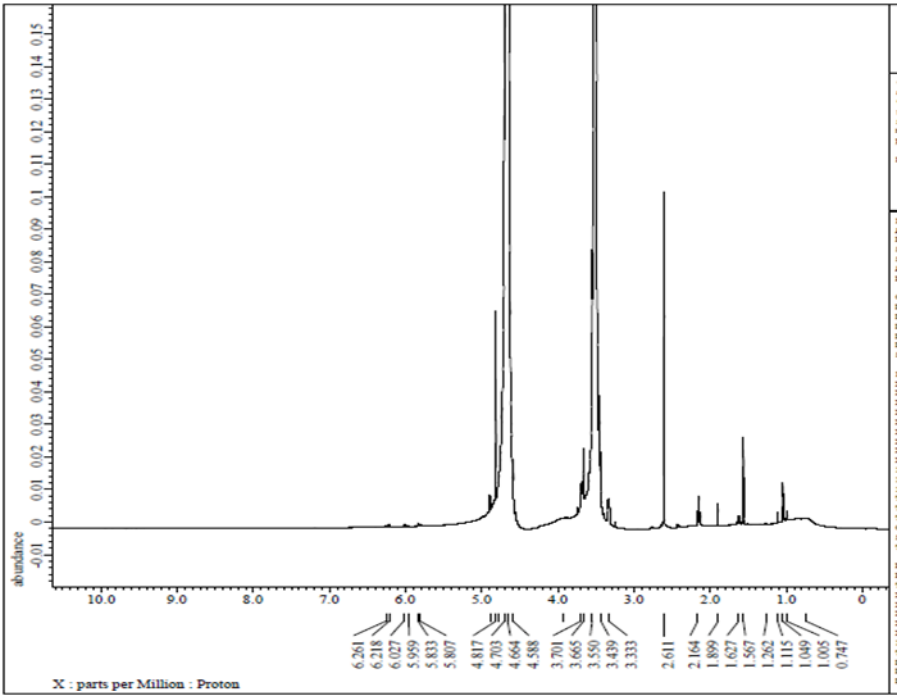

XRD

PCEs mixed with Na-Bentonite and X-ray diffraction measurements were made between 2θ=5°-70° and are given in Figure 5. The d values were calculated using the formula λ = 2.d.sinΘ. While the interlayer spacing of pure Na-bentonite was d = 1.30 nm (2Θ = 6.760), the interlayer spacing of synthesized PCE impregnated Na-bentonite was calculated as d = 1.69 nm (2Θ =5.20). The increase in the interlayer spacing in Na-Bentonite shows that the water requirement in the concrete decreases and the positive effect on the compressive strength is due to this.

Figure 5. Pure Na bentonite and Na bentonite with PCE XRD diagrams

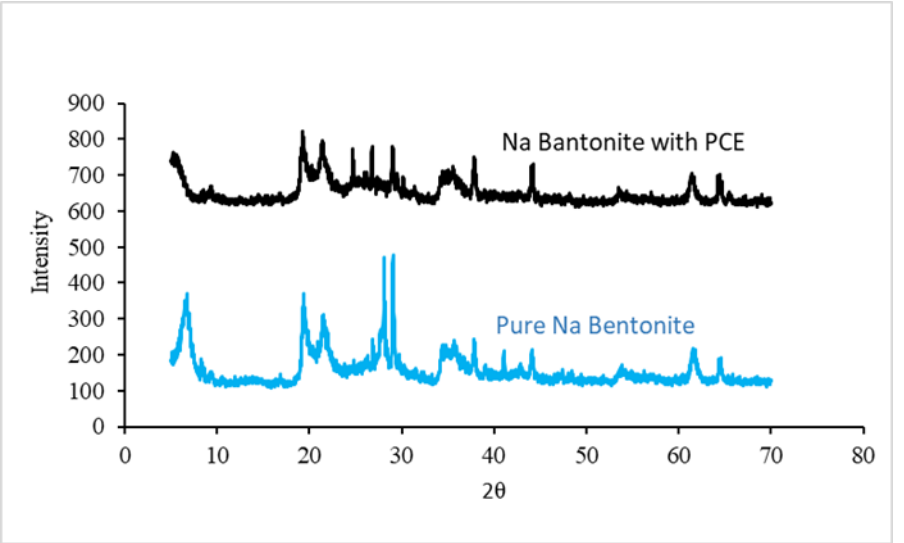

CONCLUSIONS

The concrete test results obtained with PCE synthesized with 4 hours of synthesis time, 75% IPEG ratio and 40 0C reaction temperature were determined as initial slump 18 cm, 30 min slump 15 cm, 7-day compressive strength 27.9 MPa and 28-day compressive strength 39.4 MPa. These results show that we can produce concrete with consistency class S3 and compressive strength C35/45 with the synthesized PCE. It has been shown that the synthesized PCE contributes to the decrease in water/cement ratio, consistency protection and compressive strength. The synthesized PCE caused an increase in concrete quality and provided lower cost and energy savings since it was carried out at a lower temperature.

References

Lei, L., Plank, J. (2014). Synthesis and Properties of a Vinyl Ether-Based Polycarboxylate Superplasticizer for Concrete Possessing Clay Tolerance. *Industrial and Engineering Chemistry Research, 53*, 1048-1055.

Liu, X., Wang, Z., Zhu, J., Zheng, Y., Cui, S., Lan, M., & Li, H. (2014). Synthesis, characterization and performance of a polycarboxylate superplasticizer with amide structure. *Colloids and Surfaces A: Physicochemical and Engineering Aspects, 448*, 119-129. doi: 10.1016/j.colsurfa.2014.02.022

Plank, J., Pöllmann, K., Zouaoui, N., Andres, P. R., & Schaefer, C. (2008). Synthesis and performance of methacrylic ester based polycarboxylate superplasticizers possessing hydroxy terminated poly(ethylene glycol) side chains. *Cement and Concrete Research, 38*(10), 1210-1216.

Tan, H., Gu, B., Guo, Y., Ma, B., Huang, J., Ren, J., . . . Guo, Y. (2018). Improvement in compatibility of polycarboxylate superplasticizer with poor-quality aggregate containing montmorillonite by incorporating polymeric ferric sulfate. *Construction and Building Materials, 162*, 566-575. doi: https://doi.org/10.1016/j.conbuildmat.2017.11.166

Tan, H., Guo, Y., Ma, B., Li, X., & Gu, B. (2017). Adsorbing behavior of polycarboxylate superplasticizer in the presence of the ester group in side chain. *Journal of Dispersion Science and Technology, 38*(5), 743-749.

CHAPTER 3

INVESTIGATION OF THE THERMAL AND PHYSICAL PROPERTIES OF AEROGELS PRODUCED BY THE SOL–GEL METHOD

1. Mehmet Zerrakki IŞIK[1]
2. Hasan OKTAY[2]

Introduction

Since the beginning of humanity, energy has been indispensable for sustaining life. Initially, the sources of energy, methods of acquisition, and conditions of use were not considered particularly important; however, over time, these factors have become critically significant. Increasing resource efficiency is essential to maintaining social and industrial stability. In this context, insulation plays a key role in heat transfer systems across various applications. The primary function of insulation is to enable systems to operate closer to their optimum performance by reducing the effects of external environmental factors. This requirement applies

[1]Assoc. Prof. Dr., Batman University, Dept. of Mechanical Engineering, Orcid: 0000-0001-9753-6458
[2]Assist. Prof. Dr., Batman University, Dept. of Mechanical Engineering, Orcid: 0000-0002-0917-7844

to both industrial processes and the air conditioning of living spaces to ensure thermal comfort.

Porous materials, widely used in insulation systems, are also employed in other applications due to their high specific surface areas. These areas include adsorption, catalysis, support materials, supercapacitors, catalyst production, separation technologies, pharmaceutical manufacturing, environmental remediation, desalination, water treatment, optical sensors, and electronic and magnetic devices. Both synthetic and natural porous materials—such as activated carbon, zeolites, silicates, polymers, and inorganic hybrid materials—fall within this scope (Enes, 2019).

Aerogels are the lightest known solid materials, with porosities of approximately 95%. Recent technological advances have increased interest in high-performance materials such as aerogels. Their low density, large surface area, low thermal and electrical conductivity, and advantageous optical and acoustic properties make them ideal for applications such as insulation, storage and transport media, sensors, catalysts, ion exchange, and separation systems. Due to their exceptional thermal and electrical insulation properties, they are often referred to as superinsulators (Mermer, 2018).

Aerogels are classified into various types, including carbon, silica, alumina, metal, and nanotube aerogels. Among these, silica aerogels are the most widely used because they are produced from natural raw materials and are environmentally friendly. They are well known for their excellent properties, such as high surface area, high porosity, low density, and low dielectric constant (Saraç, 2018).

Advances in technology have led to the emergence of new application areas for these materials. Silica aerogels are typically produced via the sol–gel process under acidic or basic conditions, using either pure silicon sources or waste materials. Although some

studies have reported the synthesis of silica aerogels from waste materials such as fly ash, rice husk ash, and corn cob ash, most research has focused on aerogel synthesis from precursors such as tetraethyl orthosilicate (TEOS) and tetramethyl orthosilicate (TMOS) (Mermer, 2018).

For the production of silica aerogels, the supercritical CO_2 drying method developed by L. Berkeley has been widely investigated. This method involves replacing the liquid CO_2 within the aerogel with alcohol under controlled pressure and temperature conditions. Under these conditions, the fluid—being in a supercritical state at CO_2's critical point of 75 bar pressure and 32 °C temperature—is removed without generating capillary stresses. Its low critical temperature and non-flammable nature, unlike conventional high-temperature and high-pressure alcohol-based techniques, help prevent structural damage during supercritical drying (Gürsoy, 2019).

Previous studies have demonstrated that silica aerogels can be produced via the sol–gel method at atmospheric pressure and 40 °C. Characterization results showed that aerogels produced by this method had a bulk density of 0.33 g/cm³, a porosity of 87%, a total pore volume of 3.31 cm³/g, an average pore diameter of 26.5 nm, and a surface area of 500 m²/g (Li & Wang, 2008; Yılmaz, 2013).

In one study (Gao et al., 2016: 405), the use of aerogel-based glazing in energy-efficient buildings was examined by evaluating energy performance, economic feasibility, and environmental impacts. By integrating aerogel granules into the air gap of double-glazed units, low thermal transmittance values were achieved. Although significant improvements were obtained in thermal and acoustic insulation, a considerable reduction in mechanical strength was also observed. In another study (Gao, Jelle & Gustavsen, 2016: 723), it was demonstrated that aerogel glazing could be effectively used on building façades. The authors also emphasized the

importance of addressing architectural challenges, durability, aesthetics, and environmental impacts. The existing literature suggests that energy losses originating from building façades—particularly from windows, which account for approximately 45% of total losses—can be significantly reduced by using glazing systems with low thermal transmittance.

This study focuses on the production of aerogel-based insulation materials with low bulk density and high thermal insulation performance, synthesized using different chemical methods. The main objective of the study is to help reduce Türkiye's dependence on imported energy by developing domestically produced materials that provide superior thermal insulation for industrial and construction applications.

Aerogel Production Methods

Silica aerogels are three-dimensional nanostructured materials composed of a cross-linked SiO_2 network. The pore diameters in silica aerogels typically range from 2 to 50 nm, classifying them as mesoporous materials. The main properties of silica aerogels are summarized in Table 1. These materials are produced via a two-step sol–gel process, a complex chemical synthesis technique that forms ceramic oxides from solution. During this process, silica aerogels are formed using organosilicon precursors and subsequently dried by supercritical extraction. This drying method prevents the collapse of the fragile pore network by removing the liquid phase without crossing the liquid–gas boundary (Sıyın, 2016).

Table 1. *General properties of silica aerogels*

Property	Value
Density	0.003 g/cm³
Surface Area	500–1000 m²/g

Porosity	80–99.8%
Pore Diameter	20–150 nm
Primary Particle Diameter	2–5 nm
Thermal Conductivity	0.015–0.018 kcal/m.h.°C
Coefficient of Thermal Expansion	$2.0–4.0 \times 10^{-6}$
Speed of Sound	100 m/s
Dielectric Constant	1.1
Refractive Index	1.0–1.05

Source: Sıyın, 2016, Hwang & Hyun, 2004: 238

The gels produced during synthesis exhibit both liquid and solid characteristics and are classified according to the drying method employed. When dried by evaporation at ambient pressure, the resulting material is referred to as a xerogel or ambigel. If supercritical drying is used, the material is classified as an aerogel, while freeze-dried samples are known as cryogels (Figure 1).

Figure 1. *Types of aerogels according to drying technique*

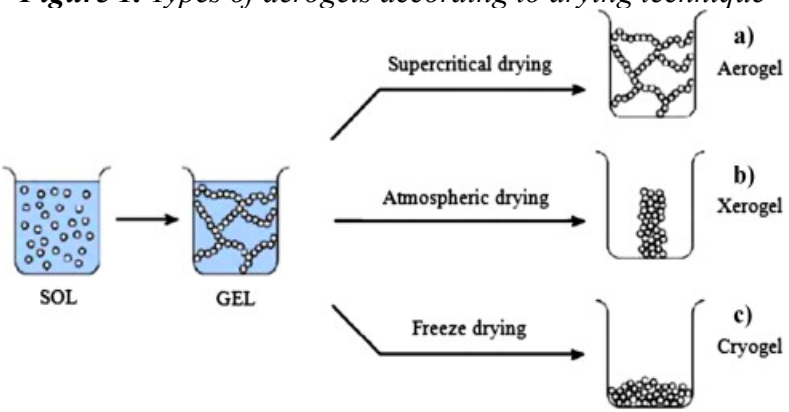

Source: García-González et al., 2012: 297

Gels can be classified according to the solvent used in their synthesis. Alcohol-based gels are referred to as alcogels, water-based gels as hydrogels, and acetone-based gels as acetogels. After drying, all of these gel types can be classified as aerogels. The term

“aerogel” derives from their air-filled porous structure. Table 2 summarizes the applications of aerogels and the properties that make them suitable for these purposes.

Table 2. *Properties and application areas of aerogels*

Property Category	Key Characteristics	Main Application Areas
Thermal Properties	Low thermal conductivity, high insulation performance, low density, transparent structure, resistance to high temperatures	Building and architectural thermal insulation, household appliance insulation, portable cooling systems, vehicles, pipelines, skylights, spacecraft and satellites, casting molds
Structural Properties	High porosity, low density, structural homogeneity, large specific surface area, multicomponent structure	Catalytic systems, adsorbent and sorbent materials, sensors, fuel storage systems, ion exchange media, X-ray laser applications
Optical Properties	Low refractive index, high optical transmittance, compositional flexibility	Cherenkov detectors, lightweight optical components, special-purpose optical systems
Acoustic Properties	Low sound propagation velocity	Impedance-matching elements in power transducers, distance measurement systems, and loudspeaker components
Mechanical Properties	Elastic behavior, low weight	Energy-absorbing structures, hypervelocity particle impact systems
Electrical Properties	Low dielectric constant, high dielectric strength, large surface area	Vacuum electrode separators, capacitor components

Source: Sıyın, 2016

Advantages and disadvantages of the sol–gel process

The advantages of the sol–gel process are as follows:

- It provides molecular-level homogeneity through the use of liquid precursors.
- It operates at low temperatures, facilitating the incorporation of organic molecules and dyes.
- It employs environmentally friendly production methods, utilizing simple equipment and atmospheric conditions.
- It enables the fabrication of materials with tailored pore sizes and high mechanical stability.
- The low viscosity of the solution allows for the easy production of thin films.
- It allows materials to be produced in various physical forms (Sıyın, 2016; Lin & Ritter, 1997).

The disadvantages of the sol–gel process are as follows:

- Significant shrinkage occurs during gelation and drying.
- Structural instability may arise if the pore size distribution is not carefully controlled.
- Drying processes can lead to high production costs.
- In addition, the removal of residual hydroxyl and organic groups is challenging (Sıyın, 2016; Lin & Ritter, 1997).

Mechanism of silica aerogel production

In the sol–gel process, metal alkoxide precursors consist of a central metal atom bonded to alkyl groups known as ligands. In silica aerogel synthesis, the most common alkyl groups are methyl and ethyl groups bonded to tetrafunctional silicon atoms. The most frequently used silica precursors are tetraethyl orthosilicate (TEOS) and tetramethyl orthosilicate (TMOS), with molecular formulas $Si(OC_2H_5)_4$ and $Si(OCH_3)_4$, respectively. Silica aerogels are typically synthesized through five main stages:

1. Hydrolysis
2. Condensation
3. Aging
4. Solvent exchange and surface modification
5. Drying (Figure 2)

Figure 2. *Schematic representation of silica aerogel synthesis via the sol–gel method*

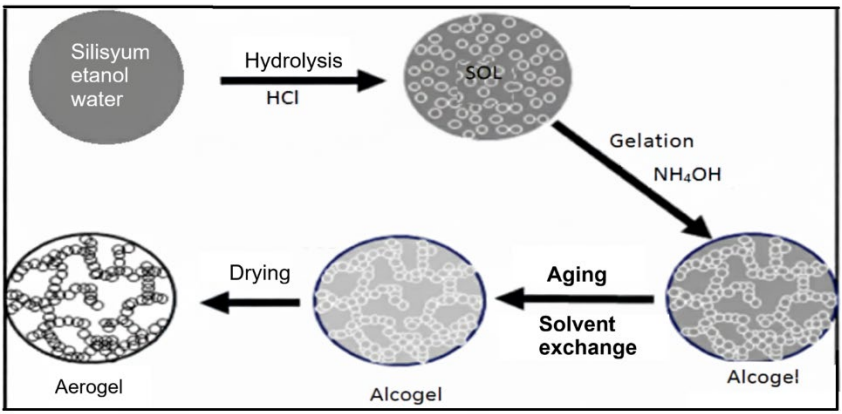

Source: Sanli & Erkey, 2013: 11708

Understanding the chemical reactions and mechanisms underlying the sol–gel process is essential for producing aerogel composites. Silicon atoms bonded to four alkoxide groups form a symmetric tetrahedral structure that eliminates dipole moments, rendering the precursor nonpolar and immiscible with water. Therefore, a co-solvent that is compatible with both the precursor and water is required to facilitate hydrolysis.

During hydrolysis, colloidal particles remain suspended in the solvent, and the rates of nucleation and growth influence their size. When nucleation is dominant, small colloidal particles form and bind via chemical bonds, hydrogen bonding, or van der Waals

interactions to create a three-dimensional gel network. Because unreacted species remain present, hydrolysis and condensation reactions continue even after gel formation (Du, Wang & Chen, 2009).

Condensation reactions initially form dimers, followed by trimers, and ultimately larger structures, resulting in an interconnected network. The condensation rate reaches its minimum at pH 1.5 and attains a maximum near pH 7 (Özdemir, Akın & Yıldırım, 2004).

Aging and drying processes

Aging refers to the period between gel formation and solvent removal. During this stage, condensation reactions continue, strengthening the gel network and increasing its stiffness and mechanical strength. This process is necessary to enhance the stability of aerogels (Pekala, 1989: 3221).

Drying is the most critical stage in aerogel production. Solvent removal generates capillary stresses that can cause collapse of the pore structure, particularly in materials with nanoscale pores. This degradation is more pronounced in smaller pores, as the resulting capillary stresses are inversely proportional to pore size (Pekala, 1989: 3221; Baetens et al., 2010: 147; Leventis et al., 2002: 957). Consequently, ambient drying of alcogels—where solvent removal occurs primarily by evaporation—results in significant shrinkage and substantial structural changes within the gel.

The primary drying methods include freeze drying, supercritical drying, and ambient-pressure drying. Freeze-drying involves sublimating the solvent from a frozen gel. The freeze-drying process consists of three main stages: first, the material is completely frozen; second, primary drying is performed; and finally, secondary drying completes the process (Labconco Corporation, 2009).

Supercritical drying is one of the most effective and least damaging drying techniques, as it eliminates phase boundaries within the pores and the associated capillary stresses. The wet gel, whose pores typically contain alcohol, is brought into contact with a solvent under supercritical conditions. As a result, the pore liquid dissolves in the supercritical fluid, forming a single-phase binary mixture. A continuous flow of the supercritical fluid removes pore liquid from the structure. In the final stage, the system pressure is reduced, converting the fluid within the pores into the gas phase. Because no phase boundary forms during the process, solvent removal is achieved without causing structural damage to the aerogel (Pekala, 1989: 3221; Leventis et al., 2002: 957).

In supercritical drying applications, carbon dioxide (CO_2) is the most commonly used fluid due to its low critical temperature and pressure, non-toxicity, and high solvating power. Although alternative supercritical fluids have been reported in the literature, their use is limited by safety and energy requirements. The stages of the CO_2 supercritical process are illustrated in Figure 3.

Figure 3. *Supercritical CO_2 low-temperature drying process*

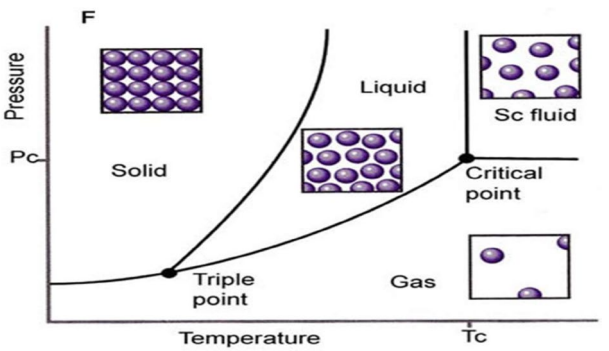

Source: Dorcheh. & Abbasi 2008: 10

The production of aerogels under supercritical conditions entails significant disadvantages, including high costs, the need for high pressures, and the risk of flammable or explosive conditions.

To mitigate these drawbacks, improve process safety, and reduce costs, ambient-pressure drying methods have been increasingly adopted in recent years, with successful results reported in the literature (Pekala, 1989: 3221). However, the most critical limitation of this method is the capillary forces that develop on the pore walls during evaporation. These forces can lead to shrinkage and partial collapse of the gel structure (Özdemir, Akın & Yıldırım, 2004: 145).

Materials and Methods

Aerogel synthesis begins with the formation of a porous, liquid-filled gel structure. Aerogels are produced by replacing the liquid within these pores with air while preserving the stability of the gel network. In this study, a two-step sol–gel process was employed to tailor the aerogel's microstructure and to leverage combined base-catalyzed hydrolysis.

Initially, tetramethyl orthosilicate (TMOS) was used as the silica precursor, and ammonium hydroxide (NH_4OH) was employed as the base catalyst. The initial conditions were determined by reviewing similar studies in the literature. In the second stage, tetraethyl orthosilicate (TEOS) was used as the silica source, and in addition to the NH_4OH catalyst, ammonium fluoride (NH_4F) was also introduced. The effects of different synthesis parameters on aerogel formation were systematically investigated.

Starting materials

The materials used in the production of silica aerogels, along with their properties, are listed below. Sigma-Aldrich supplied all chemicals:

- TEOS ($Si(OC_2H_5)_4$): Serves as the silica source for aerogel synthesis. Also known as tetraethyl orthosilicate, TEOS is an organosilicon compound widely used in sol–gel processes.

- TMOS ($Si(OCH_3)_4$): Used as a silica precursor in aerogel synthesis. Tetramethyl orthosilicate is a chemical compound containing four methoxy groups bonded to a silicon atom.
- Ammonium hydroxide (NH_4OH): Used as a base catalyst in silica aerogel production; it is an aqueous solution of ammonia.
- Ammonium fluoride (NH_4F): Employed as a catalyst to accelerate hydrolysis reactions through the action of fluoride ions.
- Methanol (CH_3OH): Used during the aging stage to remove water from the aerogel structure.
- Ethanol (C_2H_5OH): Used during the aging stage to facilitate solvent exchange and remove water from the gel structure.

Silica Aerogel Synthesis

The distinguishing feature of the silica aerogels produced in this study is that ethanol and methanol were used as hydrolysis media, while NH_4OH and NH_4F were employed as condensation catalysts. All other synthesis steps were kept constant. The experimental procedure consisted of five main stages. Initially, TMOS and TEOS were diluted in methanol and ethanol at different concentrations, and water and alcohol were added under continuous stirring using a magnetic stirrer to initiate hydrolysis. After the base catalyst was added, the condensation reaction was initiated, and the resulting solution was poured into pre-prepared 5 mL molds. The experimental stages of silica aerogel production are illustrated in Figure 4.

Figure 4. *Experimental procedure for silica aerogel synthesis using (a) tmos and (b) teos*

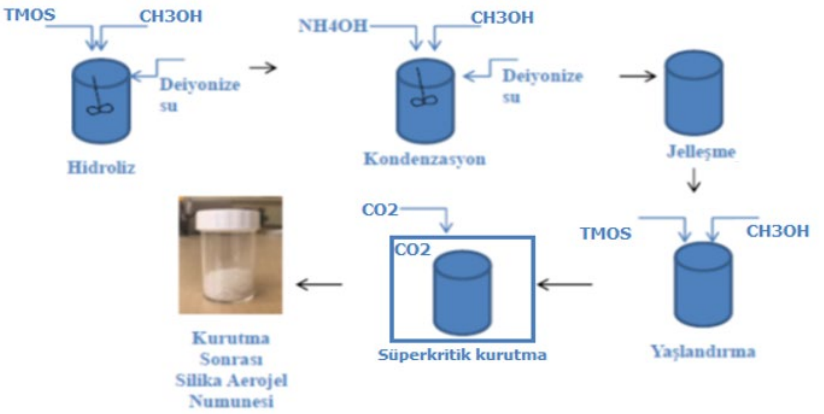

(a)

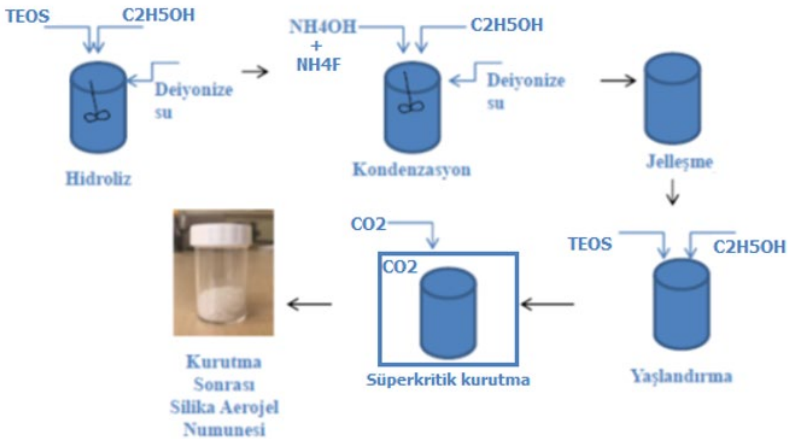

(b)

The gelation time is directly dependent on the concentrations of TMOS and TEOS in the solution. In some cases, gelation occurred only a few minutes after catalyst addition, leaving insufficient time for molding. This issue was resolved through experimental optimization by precisely adjusting both the catalyst base concentration and the rate of catalyst addition. Table 3 presents the

compositions of the samples prepared under different material and solution conditions.

Table 3. *Sample compositions based on material and solution variations*

No.	TMOS (g)	TEOS (g)	Ethanol (g)	Methanol (g)	Deionized Water (g)	NH_4OH (g)	NH_4F (g)
1	5.3	–	8.2	–	19.6	0.01	0.06
2	5.5	–	8.6	–	20.5	0.01	0.07
3	–	11.7	–	5.6	18.1	–	0.03
4	–	12.2	–	6.0	19.0	–	0.03
5	–	10.4	–	5.0	–	8.0	0.03

Production of the drying experimental setup and processes

The entire aerogel production process, including supercritical drying, was completed in approximately three days. The drying procedure was carried out by following the steps outlined below (Figure 5):

Figure 5. *Experimental setup used for supercritical drying*

Prior to drying, the molds containing the wet gels were placed into the reactor and fully immersed in alcohol to prevent premature evaporation.

- The reactor lid was securely fastened with nuts and bolts to ensure an airtight seal.
- To avoid damage to the pore structure of the gel, liquid carbon dioxide was introduced gradually by slowly opening the CO_2 valve over a period of one hour.
- Once the internal pressure of the reactor reached that of the CO_2 cylinder (55 bar), the inlet valve was closed to check for possible leakage.
- After confirming system integrity, solvent exchange between the alcohol and liquid CO_2 was carried out over two days; during this period, drying occurred primarily through the diffusion of ethanol from the gel pores.
- The system was then brought to supercritical drying conditions.
- Following supercritical drying, the aerogels were cooled to room temperature to finalize their shape. Figure 6 shows the appearance of the aerogels after the drying process.

Figure 6. *Dried circular aerogels synthesized from TEOS and TMOS*

Tests Applied to Aerogel Insulation Materials

The characterization of aerogel insulation materials was classified into two main categories: physical and thermal properties. Physical evaluations included bulk density and mass loss, whereas thermal properties were determined from thermal conductivity measurements.

Measurement of bulk density

Sol–gel and aerogel samples prepared at specified volumes were weighed using a balance with a precision of 0.01 g. The bulk density was determined by averaging the results of three samples using the following equation:

$$\rho_k = M_k / V$$

Determination of thermal conductivity coefficient

The thermal conductivity coefficients of aerogels synthesized using different chemical compositions were measured using a Thermtest analyzer. This method involves inserting a needle-shaped probe into the sample and recording the temperature at regular intervals during a controlled heating period. Following the heating phase, temperature data were also collected at the same intervals during the cooling stage. Thermal conductivity values were calculated using the following equation:

$$k = q / 4\pi a$$

where k is the thermal conductivity (kcal/m.h.°C), q is the heating power of the probe, and a represents the slope of the logarithm of temperature rise with respect to time. Measurements were conducted on six samples, and the reported results represent the mean values. The thermal conductivity coefficients of the produced aerogels were measured using the device shown in Figure 7.

Figure 7. *Determination of thermal conductivity of the produced aerogels*

Results and Discussion

Within the scope of this study, the physical and thermal properties of aerogels synthesized with varying chemical compositions were determined using appropriate testing methods. The results of the relevant tests are presented in Table 4 as average values.

Table 4*. Thermophysical properties of produced sol–gel and aerogel samples*

No.	Sol–Gel Density (g/cm³)	Aerogel Density (g/cm³)	Aerogel Thermal Conductivity (kcal/m.h.°C)
1	0.946	0.589	0.075
2	0.990	0.620	0.078
3	1.002	0.636	0.079
4	1.053	0.670	0.083
5	0.660	0.420	0.058

In this study, five different synthesis methods were employed to produce aerogels. These materials were subjected to comprehensive testing, and the collected data were systematically analyzed. The measured bulk densities ranged from 0.66 to 1.053

g/cm³, while the thermal conductivity coefficients varied between 0.058 and 0.083 kcal/m.h.°C. Compared with values reported in the literature, the aerogels produced in this study exhibited relatively higher density and thermal conductivity. This increase in density is attributed to the strengthening of the aerogel skeletal structure, as reported in the literature, which may indicate improved mechanical strength.

Although the targeted thermal and physical performance values were met mainly, the fact that all samples exhibited thermal conductivities below 0.086 kcal/m.h.°C demonstrates the suitability of the produced aerogels for thermal insulation applications. Furthermore, the results indicate that increasing the concentrations of TEOS and TMOS during sol–gel synthesis yields higher aerogel densities and, consequently, higher thermal conductivity values. To mitigate this effect, a carbon dioxide drainage line was integrated into the system to facilitate solvent removal, resulting in specific improvements in material properties. However, factors such as the requirement for high-pressure drying conditions of up to 100 bar, the lengthy and complex preparation process, and the high cost of chemical precursors limited further process optimization. These constraints highlight the need to investigate alternative drying methods to simplify production, reduce costs, and enhance the performance and scalability of aerogel materials.

References

Baetens, R., Jelle, B. P., Thue, J. V., Tenpierik, M. J., Grynning, S., Uvsløkk, S., & Gustavsen, A. (2010). Vacuum insulation panels for building applications: A review and beyond. *Energy and Buildings, 42*(2), 147–172.

Dorcheh, A. S., & Abbasi, M. H. (2008). Silica aerogel: Synthesis, properties and characterization. *Journal of Materials Processing Technology, 199*(1–3), 10–26.

Du, X., Wang, C., Li, T., & Chen, M. (2009). Studies on the performances of silica aerogel electrodes for the application of supercapacitor. *Journal of Sol-Gel Science and Technology, 15*, 561–565.

Enes A., (2019). *Silika aerojel sentezinde farklı katalizör kullanımının etkisi ve adsorpsiyon kapasitesinin belirlenmesi* (Yüksek Lisans tezi, Gazi Üniversitesi).

Gao, T., Ihara, T., Grynning, S., Jelle, B. P., & Lien, A. G. (2016). Perspective of aerogel glazings in energy efficient buildings. *Building and Environment, 95*, 405–413.

Gao, T., Jelle, B. P., & Gustavsen, A. (2016). Building integration of aerogel glazings. *Procedia Engineering, 145*, 723–728.

García-González, C. A., Camino-Rey, M. C., Alnaief, M., Zetzl, C., & Smirnova, I. (2012). Supercritical drying of aerogels using CO_2: Effect of extraction time on the end material textural properties. *The Journal of Supercritical Fluids, 66*, 297–306.

Gürsoy, M. (2019). *Bor atıklarının aerojel üretiminde değerlendirilmesi* (Yüksek Lisans tezi, Sakarya Üniversitesi).

Hwang, S. W., & Hyun, S. H. (2004). Capacitance control of carbon aerogel electrodes. *Journal of Non-Crystalline Solids, 347*, 238–245.

Labconco Corporation. (2009). A guide to freeze drying for the laboratory: An industry service publication. Kansas City, MO: Labconco Corporation.

Leventis, N., Sotiriou-Leventis, C., Zhang, G., & Rawashdeh, A. M. M. (2002). Nanoengineering strong silica aerogels. *Nano Letters, 2*(9), 957–960.

Li, T., & Wang, T. (2008). Preparation of silica aerogel from rice hull ash by drying at atmospheric pressure. *Materials Chemistry and Physics, 112*, 398–401.

Lin, C., & Ritter, J. A. (1997). Effect of synthesis pH on the structure of carbon xerogels. *Carbon*, 1271–1278.

Mermer, N. K. (2018). *Silika temelli aerojellerin sol-jel yöntemi ile sentezi ve yapısal özelliklerin incelenmesi* (Yüksek Lisans tezi, Yıldız Teknik Üniversitesi).

Özdemir, C., Akın, A. N., & Yıldırım, R. (2004). Low temperature CO oxidation in hydrogen rich streams on Pt-SnO_2/Al_2O_3 catalyst using Taguchi method. *Applied Catalysis A: General, 258*, 145–152.

Pekala, R. W. (1989). Organic aerogels from the polycondensation of resorcinol with formaldehyde. *Journal of Materials Science, 24*(9), 3221–3227.

Sanli, D., & Erkey, C. (2013). Monolithic composites of silica aerogels by reactive supercritical deposition of hydroxy-terminated poly(dimethylsiloxane). *ACS Applied Materials & Interfaces, 5*(22), 11708–11717.

Saraç, N. (2018). *Silika esaslı doğal hammadde ve atıklardan aerojel tozu üretimi ve karakterizasyonu* (Yüksek Lisans tezi, Sakarya Üniversitesi).

Sıyın, N. (2016). *Yüksek sıcaklık ısı yalıtım uygulamalarına yönelik üstün performanslı aerojel şilte sentezi ve karakterizasyonu* (Yüksek Lisans tezi, İstanbul Teknik Üniversitesi, Fen Bilimleri Enstitüsü).

Ülker, Z. (2011). *Preparation and characterization of silica aerogel polymer composites* (Master's thesis, Koç University, The Institute of Engineering and Sciences, İstanbul).

Yılmaz, Y. (2013). *Farklı başlangıç maddeleri kullanılarak sol-jel yöntemiyle monolitik silika aerojel ve silika aerojel sentezi ve karakterizasyonu* (Yüksek Lisans tezi, Ankara Üniversitesi, Fen Bilimleri Enstitüsü).

GEÇİCİ KAPAK

Kapak tasarımı
devam ediyor.